Lithium niobate photonic wires

H. Hu*, R. Ricken, and W. Sohler

Angewandte Physik, Universität Paderborn, 33098 Paderborn, Germany
**hhu@mail.upb.de*

Abstract: LN photonic wires of cross-section dimensions down to 1 × 0.73 μm^2 were fabricated by Ar milling of a single-crystalline $LiNbO_3$ (LN) film bonded to a $SiO_2/LiNbO_3$ substrate. Mode intensity distributions, propagation losses, and group indices of refraction were measured at 1.55 μm wavelength and compared with simulation results. Moreover, effective mode indices and end face reflectivities were numerically evaluated. The waveguide of 1 μm top width is the smallest LN photonic wire reported to date; it has a mode size of ~0.4 μm^2 (0.5 μm^2) only and propagation losses of 9.9 dB/cm (12.9 dB/cm) for qTM (qTE) polarization.

OCIS codes: (160.3730) Lithium niobate; (230.7370) Waveguides; (130.0130) Integrated optics; (130.3130) Integrated optics materials; (310.0310) Thin films

References and links

1. P. Rabiei, and W. H. Steier, "Lithium niobate ridge waveguides and modulators fabricated using smart guide," Appl. Phys. Lett. **86**(16), 161115 (2005).
2. D. Djukic, G. Cerda-Pons, R. M. Roth, R. M. Osgood, Jr., S. Bakhru, and H. Bakhru, "Electro-optically tunable second-harmonic-generation gratings in ion-exfoliated thin films of periodically poled lithium niobate," Appl. Phys. Lett. **90**(17), 171116 (2007).
3. A. Guarino, G. Poberaj, D. Rezzonico, R. Degl'innocenti, and P. Günter, "Electro–optically tunable microring resonators in lithium niobate," Nat. Photonics **1**(7), 407–410 (2007).
4. F. Schrempel, T. Gischkat, H. Hartung, T. Höche, E. B. Kley, A. Tünnermann, and W. Wesch, "Ultrathin membranes in *x*-cut lithium niobate," Opt. Lett. **34**(9), 1426–1428 (2009).
5. T. Takaoka, M. Fujimura, and T. Suhara, "Fabrication of ridge waveguides in $LiNbO_3$ thin film crystal by proton-exchange accelerated etching," Electron. Lett. **45**(18), 940–941 (2009).
6. G. Poberaj, M. Koechlin, F. Sulser, A. Guarino, J. Hajfler, and P. Günter, "Ion-sliced lithium niobate thin films for active photonic devices," Opt. Mater. **31**(7), 1054–1058 (2009).
7. G. W. Burr, S. Diziain, and M.-P. Bernal, "Theoretical study of lithium niobate slab waveguides for integrated optics applications," Opt. Mater. **31**(10), 1492–1497 (2009).
8. H. Yamada, T. Chu, S. Ishida, and Y. Arakawa, "Si photonic wire waveguide devices," IEEE J. Sel. Top. Quantum Electron. **12**(6), 1371–1379 (2006).
9. R. S. Weis, and T. K. Gaylord, "Lithium niobate: summary of physical properties and crystal structure," Appl. Phys., A Mater. Sci. Process. **37**(4), 191–203 (1985).
10. W. Sohler, B. Das, D. Dey, S. Reza, H. Suche, and R. Ricken, "Erbium-doped lithium niobate waveguides lasers," IEICE Trans. Electron. **E88**(C), 990–997 (2005).
11. H. Hu, R. Ricken, and W. Sohler, Large area, crystal-bonded $LiNbO_3$ thin films and ridge waveguides of high refractive index contrast, Topical Meeting "Photorefractive Materials, Effects, and Devices - Control of Light and Matter" (PR 09), Bad Honnef, Germany 2009. On the poster, presented to PR 09, a photograph of a 3 inch LNOI wafer was shown. A manuscript to describe the LNOI-technology developed is in preparation.
12. A. Boudrioua, J. C. Loulergue, F. Laurell, and P. Moretti, "Nonlinear optical properties of (H^+, He^+) - implanted planar waveguides in Z-cut lithium niobate: annealing effect," J. Opt. Soc. Am. B **18**(12), 1832–1840 (2001).
13. H. Hu, R. Ricken, and W. Sohler, "Low-loss ridge waveguides on lithium niobate fabricated by local diffusion doping with titanium," Appl. Phys. B. submitted.
14. P. G. Glöersen, "Ion beam etching," J. Vac. Sci. Technol. **12**(1), 28–35 (1975).
15. G. Carter, "The physics and applications of ion beam erosion," J. Phys. D Appl. Phys. **34**(3), 201 (2001).
16. R. Regener, and W. Sohler, "Loss in low-finesse Ti:$LiNbO_3$ optical waveguide resonators," Appl. Phys. B **36**(3), 143–147 (1985).
17. Z. M. Zhu, and T. G. Brown, "Full-vectorial finite-difference analysis of microstructured optical fibers," Opt. Express **10**(17), 853–864 (2002), http://www.opticsinfobase.org/oe/abstract.cfm?uri=OE-10-17-853.
18. Lumerical Solutions, *http://www.lumerical.com/*
19. D. Labukhin, and X. Li, "Three-dimensional finite-difference time-domain simulation of facet reflection through parallel computing," J. Comput. Electron. **4**(1-2), 15–19 (2005).

#118299 - $15.00 USD Received 7 Oct 2009; revised 14 Dec 2009; accepted 14 Dec 2009; published 18 Dec 2009

20. T. Ikegami, "Reflectivity of mode at facet and oscillation mode in double heterostructure injection lasers," IEEE J. Quantum Electron. **8**(6), 470–476 (1972).
21. H. A. Jamid, and M. Z. M. Khan, "3-D full-vectorial analysis of strong optical waveguide discontinuities using Pade approximants," IEEE J. Quantum Electron. **43**(4), 343–349 (2007).
22. F. Grillot, L. Viv, S. Laval, and E. Cassan, "Propagation loss in single-mode ultrasmall square silicon-on-insulator optical waveguides," J. Lightwave Technol. **24**(2), 891–896 (2006).
23. E. Dulkeith, F. N. Xia, L. Schares, W. M. J. Green, and Y. A. Vlasov, "Group index and group velocity dispersion in silicon-on-insulator photonic wires," Opt. Express **14**(9), 3853–3863 (2006), http://www.opticsinfobase.org/abstract.cfm?URI=oe-14-9-3853.
24. A. Sakai, G. Hara, and T. Baba, "Propagation characteristics of ultrahigh-Δ optical waveguide on silicon-on-insulator substrate," Jpn. J. Appl. Phys. **40**(Part 2, No. 4B 4B), L383–L385 (2001).
25. D. Duchesne, P. Cheben, R. Morandotti, B. Lamontagne, D.-X. Xu, S. Janz, and D. Christodoulides, "Group-index birefringence and loss measurements in silicon-on-insulator photonic wire waveguides," Opt. Eng. **46**(10), 104602 (2007).
26. D. E. Zelmon, D. L. Small, and D. Jundt, "Infrared corrected Sellmeier coefficients for congruently grown lithium niobate and 5 mol. % magnesium oxide-doped lithium niobate," J. Opt. Soc. Am. B **14**(12), 3319–3322 (1997).

1. Introduction

Strongly guiding Lithium Niobate ($LiNbO_3$, LN) channel waveguides of high refractive index contrast have attracted growing interest during the last years [1–7]. They enable ultra-small waveguide cross-sections below 1 μm^2 (photonic wires) and bending radii smaller than 10 µm, enabling the development of ultra-compact photonic integrated devices and circuits. In contrast to photonic wires in silicon on insulator (SOI) [8], LN offers excellent electro-optic, acousto-optic, and nonlinear optical properties [9]; moreover, it can be easily doped with rare-earth ions to get a laser active material [10]. Therefore, LN photonic wires will enable the development of a wide range of active integrated devices. They comprise electro-optical modulators, tuneable filters, nonlinear wavelength converters, and amplifiers and (tuneable) lasers of different types. Due to high mode intensities even at moderate optical power levels, devices of high efficiency can be expected.

Up to now, LN photonic wire structures of cross-section dimensions down to $2 \times 0.6\ \mu m^2$ have been reported, however, without loss data [6]. Somewhat earlier, propagation losses of 4 cm^{-1} (17 dB/cm) were observed in a similar structure, but of larger dimensions ($4 \times 0.6\ \mu m^2$) [3]. They were fabricated using "smart-cut" LN layers bonded to BCB on a LN substrate [3,6]. Using such waveguides, even tuneable ring resonators have been developed [3].

Despite these impressive results, further progress is needed to develop smaller photonic wires of better passive waveguide properties comparable with those of SOI-based structures. Only then a full exploitation of the electro-optic and nonlinear properties of LN photonic wires will be possible. Therefore, we used "LNOI" (LN on Insulator) samples as starting material to fabricate LN photonic wires. "LNOI" was recently developed a full wafer technology (3 inch diameter) analogous to the fabrication of SOI wafer [11]. It consists of a single crystalline LN layer crystal bonded to a SiO_2 layer deposited by plasma enhanced chemical vapour deposition (PECVD) on Z-cut LN. In contrast to the BCB bonded material, annealing at much higher temperatures is possible. This is important to minimize ion-implantation induced material damage and to recover in this way electro- and nonlinear optical properties [12]. Moreover, high temperature annealing contributes significantly to a reduction of the surface roughness of LN ridge guides [13].

In this paper we report the fabrication and optical characterization of LN photonic wires of a cross-section down to ~1 μm^2 using directly bonded LNOI of 730 nm LN thickness as starting material. Photonic wires of 1-7 µm top width were photolithographically defined and fabricated by Ar-milling. Mode intensity distributions, propagation losses, and group indices of refraction were measured at 1.55 µm wavelength and, whenever possible, compared with simulation results. Moreover, effective mode indices and end face reflectivities were numerically evaluated. The structures with a top width of 1 µm and mode cross sections of

#118299 - $15.00 USD Received 7 Oct 2009; revised 14 Dec 2009; accepted 14 Dec 2009; published 18 Dec 2009

~0.4 μm^2 are the smallest LN photonic wires reported to date; they have propagation losses of 9.9 dB/cm only (quasi TM polarization).

2. Fabrication

For the fabrication of LN optical wires a LNOI sample was used (see Fig. 1). It consists of a 730 nm thick single crystalline LN layer direct bonded to the surface of a 1.3 µm thick SiO_2 layer deposited by plasma enhanced chemical vapour deposition (PECVD) on the –Z-face of a congruent Z-cut LN substrate. The thin bonded LN layer has the same crystal orientation as the substrate; its surfaces have a rms-roughness of 0.5 nm obtained by chemical-mechanical polishing (CMP). Recently, the development of full LNOI wafers of a diameter of 3 inch has been reported [11].

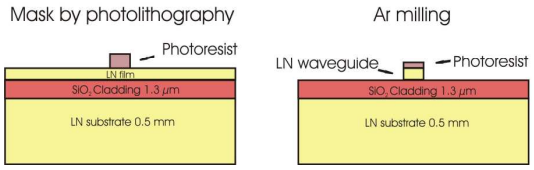

Fig. 1. Schematic diagrams of the cross-section of the LNOI sample (left) used to fabricate LN photonic wires (right) by Ar-milling.

Due to their high index contrast (n_{LN} ~2.2, n_{SiO2} ~1.44), LNOI samples are strongly guiding planar waveguides ideally suited for the fabrication of LN optical wires. Photoresist (OIR 907-17) stripes of 1.7 µm thickness and 1 - 7 µm width were used as etch mask, defined by photolithography. To improve the etching selectivity, the resist was annealed at 120 °C for 1 hour. Subsequently, the sample was etched by Ar milling for 60 min in an Oxford Plasmalab System100 with 100 W RF power inductively coupled into the plasma (ICP) and 70 W RF power coupled to the sample table. The resulting etch depth was 460 nm. Figure 2 shows scanning electron microscope (SEM) pictures of a ridge guide of 1 µm top width. The dark stripe underneath is the SiO_2 cladding. On both sides of the ridge, etched trenches can be observed, resulting from additional etching by ions reflected by the angled walls of the ridge [14]. Their slope of ~27° (with respect to the vertical direction) is determined by the dependence of the etching rate on the incident angle of the ion beam [15]. As the etched trenches seemed to isolate the ridge, a longer etching time was not considered. However, it should be possible to completely remove the remaining LN layer by an extended etching time. Finally, the end faces of the sample were carefully polished to enable efficient end-fire coupling of light; the length of the sample was 3 mm.

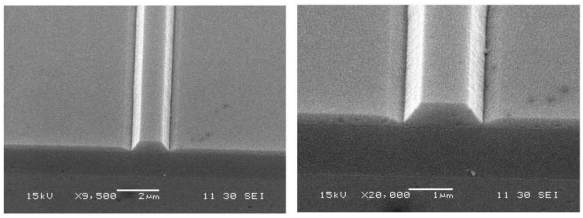

Fig. 2. SEM pictures of micro-channel ridge guides (photonic wires) of 1 µm top width. The trenches on both sides of the ridges reach near the surface of the SiO2 buffer layer.

3. Optical properties

The LN photonic wires were carefully characterized around 1.55 µm wavelength. To be specific, their mode distributions were measured and compared with modeling results. The mode propagation losses were determined for different wire width and as function of the polarization using the resonator method [16]. A correct analysis required the knowledge of the waveguide end face reflectivity, which was evaluated for a number of parameters. Moreover,

#118299 - $15.00 USD Received 7 Oct 2009; revised 14 Dec 2009; accepted 14 Dec 2009; published 18 Dec 2009

the resonator method allows determining the group index of the waveguides, which was measured in this way and also compared with modeling results.

3.1 Experimental setup

A tunable laser diode was used to investigate the photonic wires. The light was coupled to the waveguides by a 60 × / 0.8 objective with an estimated (calculated) coupling efficiency of about 40% (30%) to the fundamental mode of the wire of 2 (1) µm top width. On the output side a 100 × / 0.9 objective magnified the near field distribution of the guided mode to form an image of maximum spatial resolution (~1.1 µm) on the camera. The recorded data were transmitted to a computer for further signal processing.

3.2 Mode distributions

The mode distributions were measured as function of the waveguide width and of the polarization, and compared with simulated distributions calculated with a full-vectorial finite-difference method [17,18]. The waveguide profile assumed for the calculations is indicated in Figs. 3, 4. In the following, mode distributions for the ridge guides of 2 and 1 µm top width are presented as examples.

Despite the small cross section dimensions, both structures support - according to the modeling results - not only the fundamental, but at least also the second order mode at 1.55 µm wavelength (see Figs. 3, 4). However, by a careful adjustment of the input laser beam, the fundamental mode could be selectively excited (though it was difficult to control the selective excitation with the objective of limited resolution). Moreover, the remaining thin LN films of 270 nm thickness on both sides of the photonic wires formed a planar waveguide for qTE polarization.

Figure 3 shows the measured mode distribution for quasi TE-polarization (qTE) at the output of a 2 µm wide channel (left) together with a corresponding modeling result (middle). In view of the finite spatial resolution of the imaging system, the agreement is reasonable. The calculated second order mode is displayed on the right of Fig. 3.

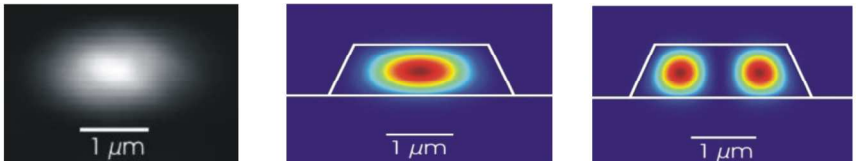

Fig. 3. Measured (left) and calculated (middle) intensity distribution of the fundamental mode in a photonic wire of 2 µm top width (qTE-polarization; λ = 1.55 µm). The intensity distribution of the simulated second order mode is shown on the right. The profile, used for the simulations, is indicated (middle and right).

Figure 4 shows the measured (left) and calculated (middle) distribution of the fundamental quasi TM mode (qTM) in a photonic wire of 1 µm top width. Again, in view of the finite spatial resolution of the imaging system, the agreement is reasonable. The extremely small area of the mode cross section is remarkable; it is about 0.4 μm^2 (product of FWHM in horizontal and vertical directions of the calculated distribution), more than one order of magnitude smaller than the mode size of about 16 μm^2 in a conventional Ti-indiffused strip guide of 7 µm width. Therefore, such photonic wires are ideal candidates to develop nonlinear devices of high efficieny. Moreover, high bending radii become possible without inducing excess bending losses. The calculated second order mode is displayed on the right. To obtain a mono-mode photonic wire, a smaller width or steeper walls are needed; e.g., by reducing the top width to 500 nm, single mode propagation can be expected.

#118299 - $15.00 USD Received 7 Oct 2009; revised 14 Dec 2009; accepted 14 Dec 2009; published 18 Dec 2009

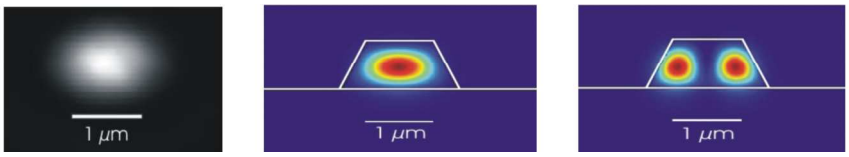

Fig. 4. Measured (left) and calculated (middle) intensity distribution of the fundamental mode in a channel waveguide of 1 μm top width (qTM-polarization; λ = 1.55 μm). The intensity distribution of the simulated second order mode is shown on the right. The profile, used for the simulations, is indicated (middle and right).

3.3 Propagation losses and end face reflectivities

As the polished waveguide end faces represent mirrors of considerable reflectivity R, waveguide cavities of low finesse are formed. By analyzing the contrast K of the cavity resonances, measured as function of the wavelength, the mode propagation losses α can be determined [16]. This method is independent on the mode excitation efficiency. α, $\widetilde{R}$ and K are defined by the following equations:

$$\alpha = \frac{4.34}{L}(\ln R - \ln \widetilde{R}) \quad \text{with} \quad \widetilde{R} = \frac{1}{K}(1-\sqrt{1-k^2}) \quad \text{and} \quad K = \frac{\mathrm{I}_{max} - \mathrm{I}_{min}}{\mathrm{I}_{max} + \mathrm{I}_{min}} \qquad (1)$$

However, due to the small waveguide cross section, the modal reflectivity R (ratio of reflected mode power to the incident mode power) can no longer be approximated by the Fresnel result for plane waves of normal incidence at a LN-air interface (~14%) as usually done for weakly guiding structures [16,19]. The actual value of R is required to enable a correct evaluation of the propagation losses. Therefore, and as a mode-selective measurement is difficult, R was calculated by a 3-dimensional finite difference time domain (FDTD) solver [18]. An auto-non-uniform mesh was used with 30 nm maximum step size in the LN waveguide region, with uniaxial perfectly matched layer (PML) boundary conditions. The result is presented in Fig. 5 as function of the top width of the ridge guides of 730 nm thickness. The slope of the ridges was kept constant. With increasing waveguide width, the end face reflectivity R approaches polarization dependent limits with a significantly higher reflectivity for qTE than for qTM. Due to the waveguide thickness of 730 nm only, the $\Delta R = R_{qTE} - R_{qTM}$ converges to ~11%; this figure shrinks to ~1% with increasing thickness, determined by the birefringence of LN alone. With decreasing waveguide width (at 730 nm thickness), ΔR also shrinks to small figures, as qTE and qTM modes become nearly degenerate [20,21].

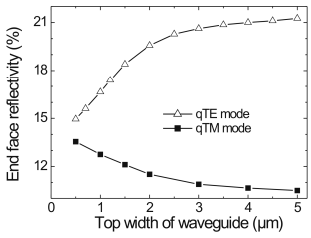

Fig. 5. Calculated end face reflectivities of the fundamental modes of qTE and qTM polarization, respectively, versus the top width of LN photonic wires of 730 nm thickness.

The simulated end face reflectivities allowed determining the waveguide propagation losses from the contrast of the cavity resonances according to the Eq. (1) given above. Figure 6 shows as example the measured normalized transmission in qTE polarization of a photonic wire of 2 μm top width as function of the wavelength (left). A propagation loss of 6.3 dB/cm was evaluated. For qTM polarization, the loss is 7.5 dB/cm. Both figures are about 10 dB smaller than the best data (17 dB/cm) reported so far for a channel guide of comparable

#118299 - $15.00 USD Received 7 Oct 2009; revised 14 Dec 2009; accepted 14 Dec 2009; published 18 Dec 2009

dimensions [3]. A corresponding result for a photonic wire of 1 µm top width, but for qTM polarization, is shown on the right of Fig. 6. The resulting propagation loss is 9.9 dB/cm. For qTE polarization, the loss is 12.9 dB/cm. The larger qTE losses in the narrower wire may result from some coupling to the planar (single polarization) waveguides on both sides of the channel.

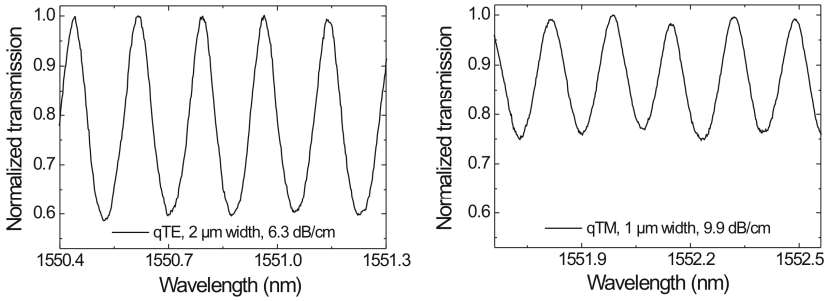

Fig. 6. Normalized transmission in qTE (qTM) polarization of a channel guide of 2 (1) µm top width as function of the wavelength (left / right).

The losses very likely arise from scattering by the residual roughness of all four walls of the ridge [22]. Losses due to a coupling of the propagating mode across the 1.2 µm thick SiO_2 layer to the substrate should be negligible (< 0.05 dB/cm), according to the calculations with a fully vectorial finite difference mode solver [18].

3.4 Effective and group indices

The waveguide mode dispersion is determined by the material dispersion of core and cladding materials and by the waveguide dimensions. Due to the high index contrast of the photonic wires and their small cross section dimensions, the effective index of refraction n_{eff} varies considerably as function of the wavelength between the bulk index of LN and that of SiO_2. It was calculated by the finite difference method for the fundamental qTE- and qTM-modes [18], respectively, and for several waveguide widths; some results are displayed in Fig. 7 together with the dispersion of bulk LN and SiO_2.

Whereas an effective mode index n_{eff} is difficult to measure, the group index n_g can be derived in a small wavelength range from the measured transmission spectra of the waveguides (see Fig. 6): $n_g = \lambda^2 / (2 \cdot L \cdot \Delta\lambda)$; L is the waveguide length and $\Delta\lambda$ is the wavelength difference of neighboring resonances [23–25]. In addition, the group index was also calculated as $n_g = n_{eff} - \lambda \cdot (dn_{eff} / d\lambda)$; measured and calculated results are shown in Fig. 7 for the fundamental modes of qTE and qTM polarization, respectively. For comparison, also the calculated group index of bulk LN is shown derived from a Sellmeier equation describing the dispersion of bulk LN [26].

#118299 - $15.00 USD Received 7 Oct 2009; revised 14 Dec 2009; accepted 14 Dec 2009; published 18 Dec 2009

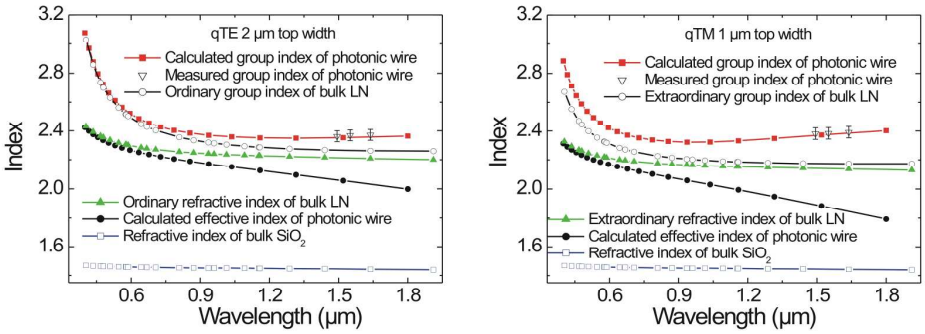

Fig. 7. Calculated effective and group indices for the fundamental modes of qTE and qTM polarization in photonic wires of 2 µm and 1 µm top widths, respectively, versus the wavelength. The measured group indices of photonic wires, the calculated group indices of bulk LN, and the refractive indices of bulk LN and SiO2 are shown as well for comparison.

The effective indices of refraction vary between the bulk indices of LN and SiO_2; the longer the wavelength and the smaller the waveguides are, the lower the effective indices become due to a decreasing mode confinement. At shorter wavelengths, the mode is more and more confined in the LN core of the waveguide and n_{eff} approaches the (polarization dependent) bulk index of LN. The group indices for light propagation in the photonic wires are substantially larger than for light propagation in bulk LN, reflecting the influence of the small waveguide dimensions. They even allow adjusting a group index dispersion close to zero in the 1.5 µm wavelength range, which is of interest for optical communication devices.

4. Conclusions

In conclusion, fabrication and optical characterization of LN photonic wires of excellent quality have been presented. Direct-bonded LNOI of 730 nm LN thickness was used as starting material; photonic wires of 1-7 µm width were photolithographically defined and fabricated by Ar-milling. Mode intensity distributions, propagation losses, and group indices of refraction were measured and, whenever possible, compared with simulation results. Moreover, effective mode indices and end face reflectivities were numerically evaluated. Remarkable are the relatively low propagation losses in the photonic wires of 1 µm top width, which are the smallest LN waveguides reported so far: 9.9 dB/cm (12.9 dB/cm) for qTM (qTE) polarization. We are confident, that by using e-beam lithography (as standard for SOI waveguides) instead of optical lithography, the propagation losses can be further reduced. And additional annealing will smooth the waveguide walls, contributing to a loss reduction as well.

Also the small mode cross sections down to ~0.4 μm^2 (in a photonic wire of 1 µm top width) are of high interest. As they are more than one order of magnitude smaller than that of conventional Ti- indiffused channel guides, nonlinear interactions of high efficiency can be expected even at low power levels. Therefore, several methods are currently explored to periodically pole the photonic wires, enabling quasi phase matching of second order nonlinear effects. PPLN photonic wires are ideal candidates for the development of a wide range of nonlinear wavelength converters and of devices for all-optical signal processing. Also modulators and Rare-Earth doped lasers would profit considerably from the high field concentration in LN photonic wires either by reduced drive voltages or lower threshold levels, respectively. Moreover, due to the high index contrast of LN photonic wires small bending radii become possible without inducing excess bending losses. A higher device integration density can be expected.

#118299 - $15.00 USD Received 7 Oct 2009; revised 14 Dec 2009; accepted 14 Dec 2009; published 18 Dec 2009

Acknowledgment

This work was funded by the Deutsche Forschungsgemeinschaft (DFG) within the framework of the project "Materials World Network: Nanoscale Structure and Shaping of Ferroelectric Domains". The authors would like to thank Dr. H. Suche, Dr. H. Herrmann, and Mr. V. Quiring for helpful discussions.

#118299 - $15.00 USD Received 7 Oct 2009; revised 14 Dec 2009; accepted 14 Dec 2009; published 18 Dec 2009